# Faster Force Transient Kinetics at Submaximal $Ca^{2+}$ Activation of Skinned Psoas Fibers from Rabbit

Donald A. Martyn* and P. Bryant Chase‡
*Center for Bioengineering and ‡Departments of Radiology and Physiology & Biophysics, University of Washington, Seattle, Washington 98195 USA

ABSTRACT The early, rapid phase of tension recovery (phase 2) after a step change in sarcomere length is thought to reflect the force-generating transition of myosin bound to actin. We have measured the relation between the rate of tension redevelopment during phase 2 ($r$), estimated from the half-time of tension recovery during phase 2 ($r = t_{0.5}^{-1}$), and steady-state force at varying $[Ca^{2+}]$ in single fibers from rabbit psoas. Sarcomere length was monitored continuously by laser diffraction of fiber segments (length ~ 1.6 mm), and sarcomere homogeneity was maintained using periodic length release/restretch cycles at 13–15°C. At lower $[Ca^{2+}]$ and forces, $r$ was elevated relative to that at pCa 4.0 for both releases and stretches (between ±8 nm). For releases of $-3.4 \pm 0.7$ nm·hs$^{-1}$ at pCa 6.6 (where force was 10–20% of maximum force at pCa 4.0), $r$ was $3.3 \pm 1.0$ ms$^{-1}$ (mean ± SD; $N = 5$), whereas the corresponding value of $r$ at pCa 4.0 was $1.0 \pm 0.2$ ms$^{-1}$ for releases of $-3.5 \pm 0.5$ nm·hs$^{-1}$ (mean ± SD; $N = 5$). For stretches of $1.9 \pm 0.7$ nm·hs$^{-1}$, $r$ was $1.0 \pm 0.3$ ms$^{-1}$ (mean ± SD; $N = 9$) at pCa 6.6, whereas $r$ was $0.4 \pm 0.1$ ms$^{-1}$ at pCa 4.0 for stretches of 1.9 ± 0.5 (mean ± SD; $N = 14$). Faster phase 2 transients at submaximal $Ca^{2+}$-activation were not caused by changes in myofilament lattice spacing because 4% Dextran T-500, which minimizes lattice spacing changes, was present in all solutions. The inverse relationship between phase 2 kinetics and force obtained during steady-state activation of skinned fibers appears to be qualitatively similar to observations on intact frog skeletal fibers during the development of tetanic force. The data are consistent with models that incorporate a direct effect of $[Ca^{2+}]$ on phase 2 kinetics of individual cross-bridges or, alternatively, in which phase 2 kinetics depend on cooperative interactions between cross-bridges.

## INTRODUCTION

A surprising feature of the mechanics of the regulated actomyosin interaction is that the transient force responses to small amplitude length steps are actually faster during the rising phase of tetanic tension than during the plateau (Bagni et al., 1988; Ford et al., 1986). When muscle length is rapidly stepped at either maximal or submaximal levels of activation, the force response consists of an instantaneous elastic phase (phase 1) followed by tension recovery on the millisecond time scale (phase 2) and subsequent slower transitions (phases 3 and 4) leading to the steady isometric level (Ford et al., 1977; Huxley and Simmons, 1971). In intact skeletal fibers, the rate of tension recovery during phase 2 increases with increasing step amplitude for releases and is slower and relatively insensitive to step amplitude after stretches (Ford et al., 1977; Huxley and Simmons, 1971). It is important to understand phase 2 and its apparent activation dependence because it is thought to reflect actomyosin dynamics, including conformational changes within attached myosin cross-bridges, which are associated with the elementary force-generating event (Ford et al., 1977; Huxley and Simmons, 1971; Irving, 1993; Irving et al., 1992; Lombardi et al., 1992).

Two potential mechanisms have been proposed to explain the apparent activation dependence of phase 2 kinetics measured during the transition from rest to steady tetanic force. The mechanism could involve the flux of cross-bridges from detached states to force-generating states during the approach to a new steady level of activation (Brenner, 1990; Ford et al., 1986). For example, phase 2 tension recovery could result from transitions between weakly and strongly attached states (Brenner, 1990) or between two sets of unstrained and strained cross-bridge states, with the first set having faster kinetics (Ford et al., 1986). Alternatively, an activation dependence of phase 2 could result from cooperative interactions between attached cross-bridges, such that the backwards rate for the force-generating transition slows as cross-bridge attachment increases (Bagni et al., 1988). One can begin to discern between these mechanisms because the first mechanism predicts no difference in the steady-state cross-bridge distribution at different activation levels, thus implying no steady-state activation dependence of phase 2 kinetics. However, these models would predict a dependence of phase 2 kinetics on the steady level of activation if at least one of the rate constants governing rapid transitions within the cross-bridge cycle were dependent upon $[Ca^{2+}]$, or if the proposed $B$ state were preferentially occupied at submaximal activation (Ford et al., 1986). Likewise, the cooperative mechanism proposed by Bagni et al. (1988) predicts that phase 2 kinetics should be faster during the non-steady-state rise of force and during steady submaximal activation, but without requiring a direct effect of $Ca^{2+}$ on cross-bridge kinetics.

To determine whether the kinetics of phase 2 vary with the steady-state level of force, we have determined the relation between the rate of tension recovery during phase 2 and force in $Ca^{2+}$-activated skinned fibers from rabbit psoas. At all

*Received for publication 20 April 1994 and in final form 8 June 1994.*
Address reprint requests to Donald A. Martyn, Ph.D., Center for Bioengineering, WD-12, University of Washington, Seattle, WA 98195. E-mail: martyn@bioeng.washington.edu.

0006-3495/95/01/235/08 $2.00

levels of activation, the rate of phase 2 tension recovery in skinned rabbit psoas fibers varied exponentially with step amplitude, being faster for releases than for stretches, as found for intact frog skeletal fibers (Bagni et al., 1988; Ford et al., 1977; Huxley and Simmons, 1971). In addition, for all amplitudes of sarcomere length change studied, phase 2 kinetics were faster at submaximal than at maximal $Ca^{2+}$-activation. Thus, because we measured phase 2 kinetics during steady-state activation, our results suggest that mechanisms involving non-steady-state flux through the cross-bridge cycle cannot explain the apparent activation dependence of phase 2 and that the kinetics of steps in the cross-bridge cycle associated with phase 2 vary with the degree of contractile activation.

A portion of these results has appeared in abstract form (Martyn et al., 1994).

## MATERIALS AND METHODS

### Fiber preparation

Segments of single muscle fibers were prepared from glycerinated rabbit psoas as described elsewhere (Chase and Kushmerick, 1988). Fiber end compliance was minimized by chemical fixation of the fiber segment ends by regional microapplication of 5% glutaraldehyde (Chase et al., 1991). To ensure destruction of membranous elements, isolated fiber segments were further treated with 1% Triton X-100 in pCa 9.2 solution for 10 min. Fiber segments were attached via aluminum foil "T"-clips (Goldman and Simmons, 1984) to small wire hooks on the mechanical apparatus; a drop of silicone sealant on the "T"-clip was used to additionally stabilize attachment to the hook. After each experiment, we determined the total length of the two chemically fixed regions at the ends of the fiber segment, as described (Chase and Kushmerick, 1988); the total fixed length was subtracted from the overall length to obtain the unfixed fiber length ($L_F$). At a relaxed sarcomere length ($L_S$) of 2.50 ± 0.02 μm (mean ± SD; $n$ = 7), $L_F$ was 1.59 ± 0.04 mm (mean ± SD; $n$ = 7) and the diameter was 57 ± 10 μm (mean ± SD; $n$ = 7). At pCa 4.0, $L_S$ decreased to 2.31 ± 0.13 μm (mean ± SD; $n$ = 7) (photomicrographs are shown in Fig. 1 *A–D* of a single fiber in relaxing solution, and partially and fully activating solutions). In our experiments, variations in sarcomere stiffness and the kinetics of phase 2 tension recovery with pCa, and thus isometric force level, could not be attributed to activation-dependent alterations in myofilament lattice spacing that occur in skinned fiber preparations (Brenner and Yu, 1985), because these force-dependent changes in lattice spacing were minimized by the presence of 4% w/v Dextran T-500 in all solutions (see Solutions) (Kawai et al., 1993; Matsubara et al., 1985). Fiber diameter was unchanged at pCa 4.0 and was 98 ± 3% (mean ± SD; $n$ = 7) of that at pCa 9.2.

### Mechanical apparatus

Force was measured with a Cambridge Technology Model 400A force transducer (peak-to-peak noise equivalent to 100 μg; resonant frequency 2.2 kHz). A Cambridge Technology (Watertown, MA) model 300 servo motor (−3 dB amplitude response at 2.4 kHz) was used to control $L_F$. $L_S$ was continuously monitored by helium-neon laser diffraction as described (Chase et al., 1993). To minimize artifacts in $L_S$ detection caused by translation, the laser beam was positioned on the fiber closer to the force transducer than to the motor. Furthermore, the region of the fiber segment that was sampled by the laser (0.8 mm beam diameter at intensity $e^{-2}$; model 05-LHR151, Melles Griot, Boulder, CO) was a significant fraction of the total length of the unfixed fiber ($L_F$ ~ 1.6 mm), thereby averaging the contribution of individual sarcomere domains (Goldman, 1987; Zite-Ferenczy et al., 1986). Steady-state $L_S$ and fiber diameter were determined at 320× magnification and were also measured from photomicrographs (400×; Fig. 1).

### Data acquisition and control

Data were acquired during continuous, steady-state activations by $Ca^{2+}$ at submaximal (pCa 6.6, 6.4, 6.2) and maximal (pCa 4.0) levels. Fiber mechanical properties and structure were maintained during activation (see Fig. 1) by using Brenner's method (Brenner, 1983; Chase and Kushmerick, 1988; Sweeney et al., 1987). Measurements of isometric force, sarcomere stiffness, and force transient kinetics were made during the steady-state period between the Brenner cycles of unloading/restretch (Brenner, 1983; Sweeney et al., 1987). The force baseline for each condition was determined unambiguously during a large amplitude, slack release. Fiber force was normalized to cross sectional area. Fiber cross sectional area was calculated from the diameter assuming circular geometry. In maximum activating $Ca^{2+}$ (pCa 4.0), the control force was 277 ± 97 $mN \cdot mm^{-2}$ (mean ± SD; $n$ = 7); relaxed force (pCa 9.2) was 1.8 ± 0.4% (mean ± SD; $n$ = 7) of the maximum $Ca^{2+}$-activated force.

Both sarcomere stiffness and kinetics of the early phase of force recovery were determined from force and $L_S$ (nm per half-sarcomere = $nm \cdot hs^{-1}$) responses to rapid, step changes in $L_F$ (Chase et al., 1993; Ford et al., 1977; Huxley and Simmons, 1971; Martyn and Gordon, 1992). Step changes in $L_F$ were implemented as 300 μs ramp changes in length. Analog signals were low-pass-filtered ($f_0$ = 4 kHz, single pole) to avoid aliasing. Signals were recorded by digitizing 2048 points with 12-bit resolution at a rate of 20 kHz per channel, with a 5 μs delay between channels. Sarcomere stiffness was determined from the slope of the relation between the maximum change in force ($T_1$) and the corresponding change in $L_S$ ($-4 < \Delta L_S < 8$ $nm \cdot hs^{-1}$) after the $L_F$ step (Chase et al., 1993). The $\Delta L_S$ intercept of this relationship ($y_0$) was obtained by extrapolation of this regression to the ordinate. Stiffness values are given as MPa ($=10^6$ $N \cdot m^{-2}$) and were obtained from the slope of the $T_1$ vs. normalized $\Delta L_S$ relation, with $T_1$ being normalized to cross sectional area and $\Delta L_S$ being normalized to the initial $L_S$.

The unprocessed, digitized data were analyzed using custom software. Reduced data were further analyzed by linear least-squares regression (Excel version 4.0 for Windows, Microsoft Corp., Redmond, WA) or by nonlinear least-squares regression (SigmaPlot version 4.1, Jandel Scientific, San Rafael, CA). Statistical analyses were performed using Excel (version 4.0 for Windows, Microsoft Corp., Redmond, WA).

### Solutions

Relaxing and activating solutions were prepared as described previously (Martyn and Gordon, 1988) and contained (in mM): 5 $Mg^{2+}$-adenosine 5′-triphosphate (MgATP), 15 phosphocreatine (PCr), 1 orthophosphate (Pi), 15 [ethylene-bis(oxyethylenenitrilo)]tetraacetic acid (EGTA), at least 40 3-[*N*-morpholino]propanesulfonic acid (MOPS), 135 $Na^+ + K^+$, 1 $Mg^{2+}$, pH 7.0, 250 $units \cdot ml^{-1}$ creatine phosphokinase (CK), and Dextran T-500 (4% w/v; Pharmacia, Piscataway, NJ). To alter solution $[Ca^{2+}]$, varying amounts of $Ca(propionate)_2$ were added as determined with a computer program, taking into account the desired free $[Ca^{2+}]$ and the binding constants of all solution constituents for $Ca^{2+}$; ionic strength was maintained constant (200 mM), by varying [MOPS] appropriately at each pCa. The experimental temperature was 13–15°C and varied by <1°C during an experiment.

## RESULTS

Force and sarcomere length responses to step changes in length were measured in single, glycerinated fibers from rabbit psoas muscle. Fiber segment length was altered within the range of ±1.1% $L_F$. Superimposed records of force (*top* panels), $L_S$ (*middle* panels), and $L_F$ (*bottom* panels) obtained during a series of length steps imposed on a single fiber segment at pCa 6.6 (*left* panels) and at pCa 4.0 (*right* panels) are illustrated in Fig. 2. The force scales at pCa 6.6 and pCa 4.0 differ, with the force axis at pCa 6.6 expanded so that the

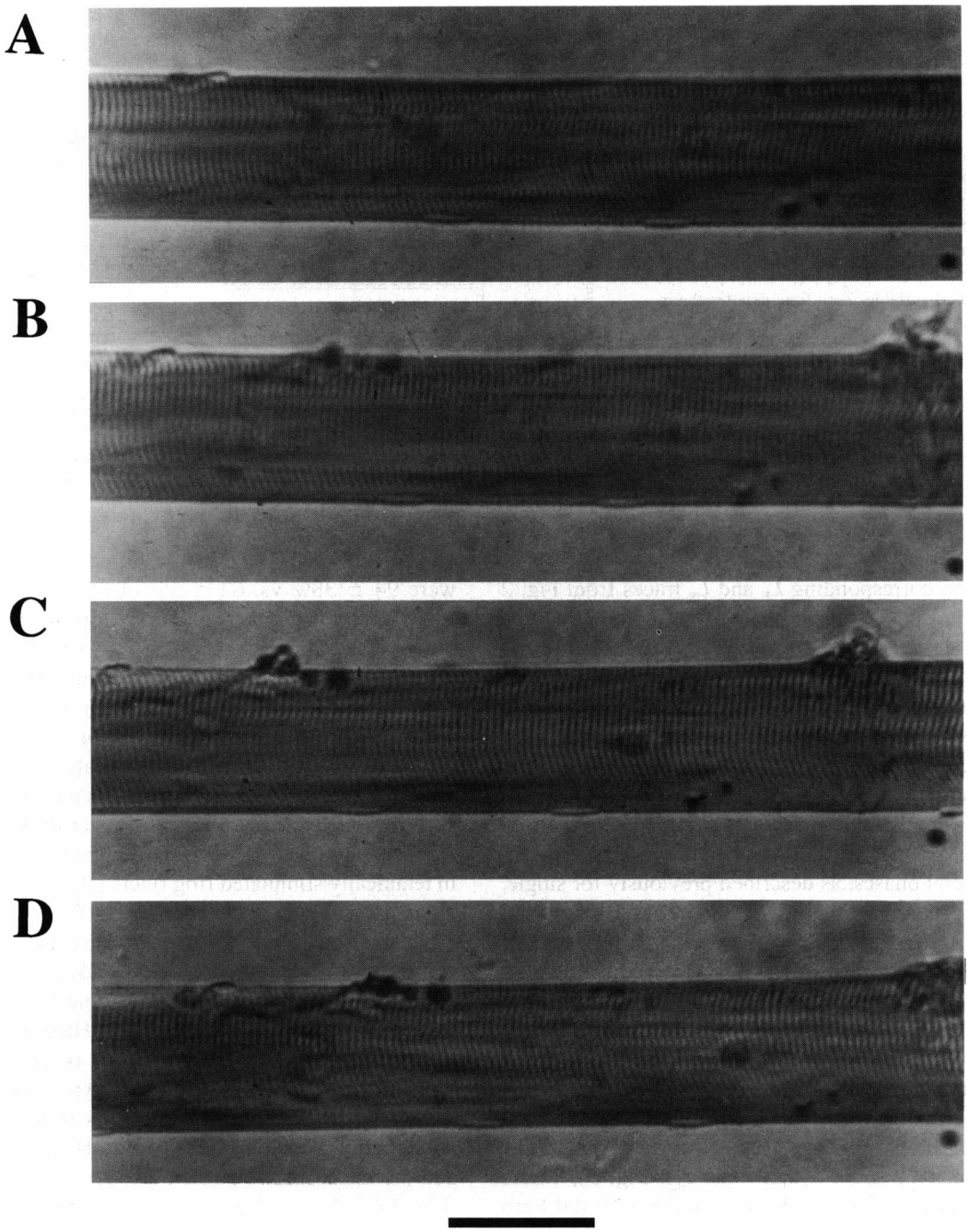


FIGURE 1 Photomicrographs of a segment of glycerinated rabbit psoas muscle fiber (*A*) in relaxing (pCa 9.2) solution, and during steady tension development at (*B*) pCa 6.6, (*C*) pCa 6.4, and (*D*) pCa 4.0. In *B*, *C*, and *D*, the fiber was photographed after 7 min of activation at each pCa and after mechanical measurements. Sarcomere length and structure were stabilized during long activations by applying periodic shortening/restretch cycles (Materials and Methods). $L_F$ was 1.64 mm. $L_S$ was (*A*) 2.52 $\mu$m at pCa 9.2, (*B*) 2.51 $\mu$m at pCa 6.6, (*C*) 2.44 $\mu$m at pCa 6.4, and (*D*) 2.39 $\mu$m at pCa 4.0. Respective fiber diameters were: (*A*) 50.6, (*B*) 49.8, (*C*) 50.1, and (*D*) 49.6 $\mu$m. The calibration bar is 50 $\mu$m.

isometric force before the length step ($t < 0$) appears to be equivalent to that at pCa 4.0. Although $L_F$ was the controlled parameter during step length changes, $L_S$ was nearly isometric both before and after the length step (Fig. 2).

Inspection of the data in Fig. 2 reveals two significant characteristics of the force transients. First, the kinetics of the tension changes after the length steps appear to be faster, for similar changes in $L_S$, at pCa 6.6 than at pCa 4.0. Second, although the absolute magnitude of force is lower at pCa 6.6 compared with pCa 4.0, the extreme excursions of force at pCa 6.6 are reduced to a lesser extent than is isometric force. The latter suggests that stiffness per unit force is higher at low $[Ca^{2+}]$, in agreement with previously published observations (Martyn and Gordon, 1992).

To illustrate more clearly the difference in tension transient kinetics at altered $[Ca^{2+}]$ levels, portions of four force

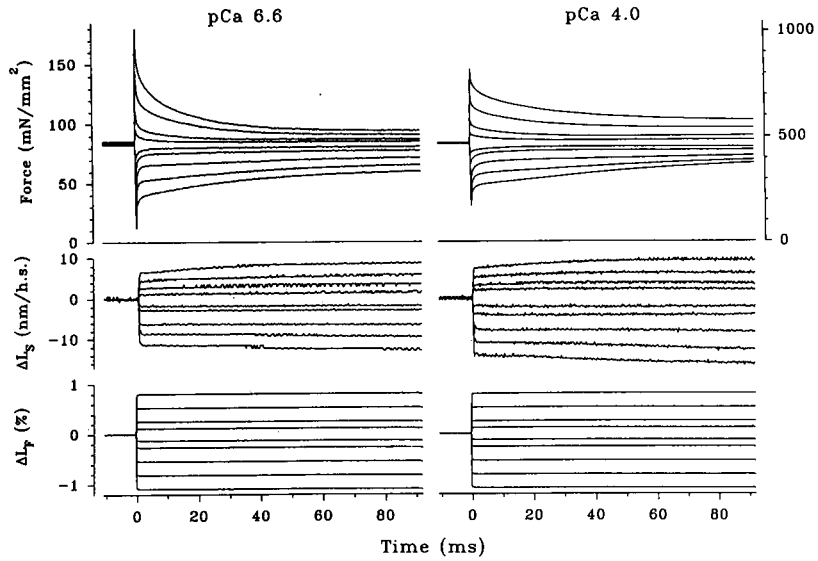


FIGURE 2 Force (*top*), sarcomere length (*middle*), and fiber segment length (*bottom*) traces obtained during a series of $L_F$ steps (−1.09 to +0.81% $L_F$) to determine stiffness at submaximal (pCa 6.6; *left* panels) and maximal $Ca^{2+}$-activation (pCa 4.0; *right* panels). $L_F$ was the feedback-controlled variable. Zero time denotes the instant that $T_1$ was measured. Note the difference in force scales at pCa 6.6 and 4.0.

records and the corresponding $L_F$ and $L_S$ traces from Fig. 2 are replotted in Fig. 3 on an expanded time scale. The force records (two stretches and two releases) were offset to superimpose isometric force and scaled such that the extreme tension excursions were equivalent. It is clear from these records that the kinetics of both tension decrease (for stretches) and early tension increase (for releases) are faster at pCa 6.6 than at pCa 4.0 (Fig. 3). To quantify this difference in tension transient kinetics, we analyzed the data according to Ford et al. (1977). Tension transients in skinned fibers exhibited several phases, as described previously for single, intact fibers from frogs (Ford et al., 1977; Huxley and Simmons, 1971). In Fig. 3, $T_1$ is the extreme tension reached during the length step (phase 1) and is followed by a partial recovery (phase 2) toward a steady force ($T_2$) before the final recovery to the isometric level of force (not shown). $T_2$ is indicated by the solid lines to the right of the corresponding force traces in the top panel of Fig. 3. The rate of the tension recovery ($r$) from $T_1$ to $T_2$ was characterized by the time required for tension to change from $T_1$ by 50% of the difference between $T_1$ and $T_2$ (half-time; $t_{0.5}$; Fig. 3), where $r = t_{0.5}^{-1}$. We chose to use $t_{0.5}$ to characterize $r$, as did Ford et al. (1977), because phase 2 tension recovery is not accurately described by a single exponential (Ford et al., 1977; Huxley and Simmons, 1971).

In Fig. 4, the dependence of $T_1$, $T_2$, and $t_{0.5}^{-1}$ on $\Delta L_S$ are shown for the data from Fig. 2. The relation between $T_1$ and $\Delta L_S$ (and thus sarcomere stiffness) at both pCa 6.6 and pCa 4.0 (Fig. 4, *A* and *B*) are similar to our previous observations (Chase et al., 1993; Martyn and Gordon, 1992). In maximum activating $Ca^{2+}$ (pCa 4.0), the control stiffness was 33 ± 18 MPa (mean ± SD; $n$ = 8 determinations on 7 fibers); relaxed stiffness (pCa 9.2) was 5.2 ± 2.5% (mean ± SD; $n$ = 8 determinations on 7 fibers) of the maximum $Ca^{2+}$-activated stiffness. At pCa 6.6, stiffness was 28 ± 13% (mean ± SD; $n$ = 6) of the maximum $Ca^{2+}$-activated stiffness, whereas force was 20 ± 3% (mean ± SD; $n$ = 6) of maximum; similarly, at pCa 6.4 normalized values of stiffness and force were 94 ± 38% vs. 62 ± 5% of maximum (mean ± SD; $n$ = 7 determinations on 6 fibers), respectively. Correspondingly, the $\Delta L_S$ intercept ($y_0$) was −9.7 ± 4.5 nm·hs$^{-1}$ (mean ± SD; $n$ = 8 determinations on 7 fibers) at pCa 4.0, −6.2 ± 1.0 nm·hs$^{-1}$ (mean ± SD; $n$ = 6) at pCa 6.6, and −6.2 ± 2.0 nm·hs$^{-1}$ (mean ± SD; $n$ = 7) at pCa 6.4.

The dependence of the apparent rate of tension recovery on $\Delta L_S$ for the data shown in Fig. 2 is plotted in Fig. 4 *C*. At both pCa 4.0 and pCa 6.6, $r$ was faster for releases than for stretches, in a qualitatively similar manner to that observed in tetanically stimulated frog fibers (Bagni et al., 1988; Ford et al., 1977; Huxley and Simmons, 1971). For a given amplitude of $\Delta L_S$, $r$ was faster at pCa 6.6 than at pCa 4.0.

The relationship between $T_1$ and $\Delta L_S$ deviates from linearity for larger releases (Fig. 4, *A* and *B*), as has been observed in intact (Ford et al., 1977; Huxley and Simmons, 1971) and skinned skeletal fibers (Chase et al., 1993; Goldman and Simmons, 1986; Martyn and Gordon, 1992). This deviation most probably results from the finite bandwidth of our force transducer (~2.2 kHz resonant frequency) and the faster rate of phase 2 tension recovery for releases (Fig. 4 *C*). As a consequence, our measurements of $y_0$ were longer than those reported by Seow and Ford (1993), who used a wider bandwidth force transducer and lower temperature (1–2°C), but are comparable with those reported previously by us (Chase et al., 1993; Martyn and Gordon, 1992). Furthermore, because the data in Fig. 4 *C* indicate that phase 2 is faster for releases at pCa 6.6 than at pCa 4.0, our analysis overestimates the value of $T_1$ and thus underestimates both the change in tension during the length step and the relative sarcomere stiffness at submaximal [$Ca^{2+}$]. For stretches, $T_1$ is underestimated, but because phase 2 tension recovery is slower for stretches than releases the degree of truncation is less than for releases. Although $T_1$ is overestimated for releases, the rate of tension recovery during phase 2 is well within the bandwidth of our force transducer.

Any force transducer causes some distortion of rapid changes in force, as would a low-pass frequency filter, and

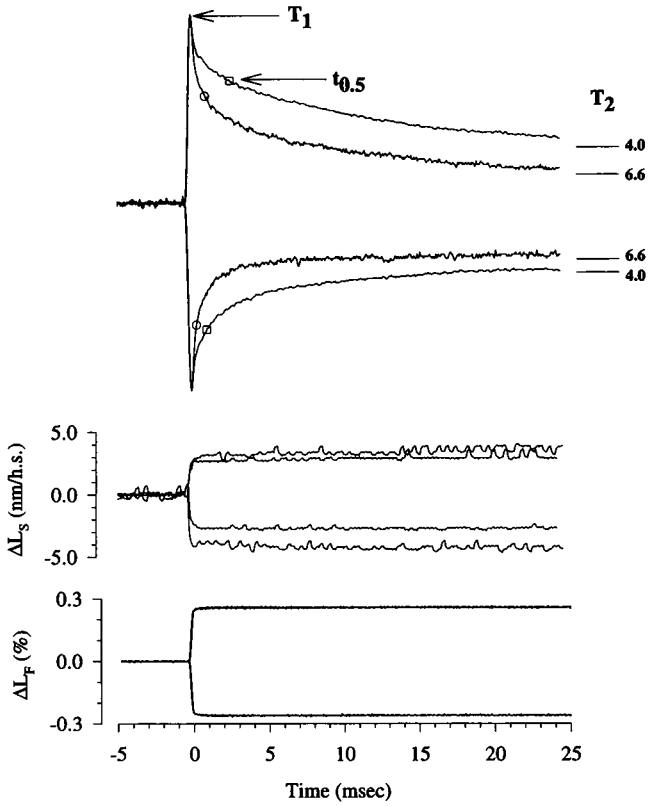


FIGURE 3 Comparison of force transients (*top*) obtained at pCa 6.6 and 4.0 (as indicated) during step stretches and releases of $L_F$ (*bottom*), with corresponding changes of $L_S$ shown in the middle panel. Stretches were 2.7 vs. 3.2 nm·hs$^{-1}$, and releases were −2.9 vs. −4.0 nm·hs$^{-1}$ at pCa 6.6 vs. pCa 4.0, respectively. To emphasize differences in tension transients, these data from Fig. 2 are shown on a faster time scale; in addition, the isometric force for each trace was subtracted and the maximum excursions in force scaled to be equivalent at each pCa. The maximum excursion of the force transients ($T_1$) is indicated for stretches by a labeled arrow, and the initial brief plateau of force approached during phase 2 ($T_2$) is indicated by solid lines at the right of each force record. Zero time was defined as the time at which $T_1$ was measured, and the time axes of $L_F$ and $L_S$ traces were corrected for electronic delays. The half-time of tension recovery ($t_{0.5}$) is indicated for pCa 6.6 (○) and pCa 4.0 (□). The values of $t_{0.5}$ for the releases were 0.37 and 0.93 ms at pCa 6.6 and 4.0, respectively; the respective values for stretches were 0.83 and 2.55 ms.

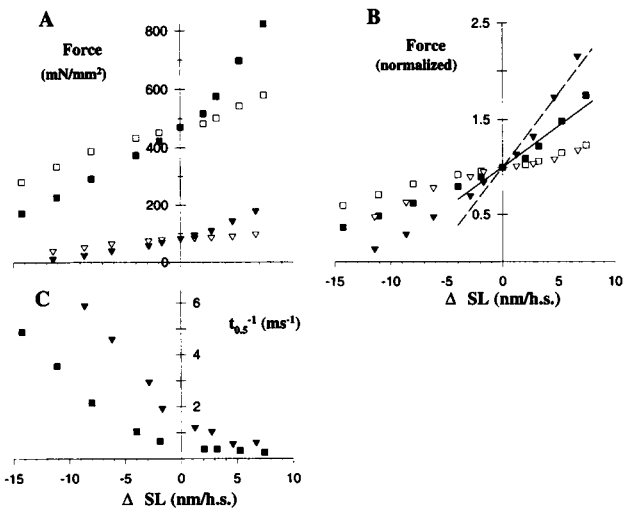


FIGURE 4 Data from ~~Fig. 2 were further analyzed to~~ determine the $\Delta L_S$ dependence of $T_1$, $T_2$ (*A*, *B*) and the rate of phase 2 tension recovery ($t_{0.5}^{-1}$) (*C*). (*A*) Values of $T_1$ (*filled symbols*) and $T_2$ (*open symbols*) obtained at pCa 6.6 (▼, ▽) and pCa 4.0 (■, □) are plotted against the corresponding $\Delta L_S$ values. Sarcomere stiffness was determined by linear regression of the values of $T_1$ and $\Delta L_S$ between −4.0 and +8.0 nm·hs$^{-1}$. At pCa 6.6, the relative values of force and stiffness were 18 and 34% of maximum, respectively; maximum force was 478 mN·mm$^{-2}$, and stiffness was 42 MPa at pCa 4.0. (*B*) Values of $T_1$ and $T_2$ were normalized to the isometric force immediately before the $L_F$ step and plotted against $\Delta L_S$. Normalized $T_1$ values obtained at pCa 6.6 (– – – –) and pCa 4.0 (——) were fit by linear regression and the $\Delta L_S$ axis intercept determined; the regression was constrained to pass through 1.0 on the ordinate. At pCa 4.0, the $\Delta L_S$ intercept was −11.7 nm·hs$^{-1}$, whereas at pCa 6.6 the corresponding value was −6.5 nm·hs$^{-1}$. (*C*) The apparent rate of phase 2 tension recovery at pCa 6.6 (▼) and 4.0 (■) is plotted against $\Delta L_S$. $t_{0.5}^{-1}$ obtained at pCa 6.6 and releases >−10 nm·hs$^{-1}$ is not shown because the rapid time course likely exceeded the bandwidth of the force transducer.

thus would have affected the calculation of $t_{0.5}$ either by truncation of $T_1$ or prolongation of the force recovery time course; either could result in an overestimation of $t_{0.5}$ and thus an underestimation of phase 2 recovery rate. However, this distortion would be more pronounced at lower levels of activation where phase 2 is faster (Fig. 4 *C*); thus, the difference in phase 2 kinetics observed between submaximal and maximal $Ca^{2+}$-activation is likely to be greater than is shown in Fig. 3. To estimate the magnitude of this distortion, we deconvolved the force records shown in Fig. 3 for the force transducer's transfer characteristics. The force transducer was characterized as a third-order, low-pass Bessel filter ($f_0$ = 2200 Hz); this characterization most closely described the frequency dependence of amplitude and phase, which was independent of steady force level, for sinusoids applied via the motor connected through a fiber fixed with 10 mM glutaraldehyde in rigor solution, after Kawai et al. (1977). The corrected $t_{0.5}$s for releases were 83 and 89% of the uncorrected values at pCa 6.6 and 4.0, respectively; for stretches, the corresponding corrected $t_{0.5}$s were 87 and 91% of the respective uncorrected traces. Thus, the observation that for a given $\Delta L_S$ $r$ was faster at lower [$Ca^{2+}$] (Fig. 4 *C*) cannot be explained by the bandwidth limitation of the force transducer, because the force transducer characteristics lead to a quantitative underestimation of the difference in $r$ at low versus high activation levels, particularly for releases where phase 2 is fastest.

The kinetics of phase 2 tension recovery were found to be faster at pCa 6.6 than at maximal $Ca^{2+}$-activation in each of seven fibers tested, and the pooled data are shown in Fig. 5. Data obtained at pCa 6.4 were intermediate between that obtained at pCa 6.6 and pCa 4.0. The relationship between $r$ and $\Delta L_S$ was analyzed as described by Huxley and Simmons (1971). The pooled data at each pCa were fit using nonlinear regression analysis to the equation

$$r = t_{0.5}^{-1} = k_{-}(1 + e^{-\alpha \cdot \Delta L_s}). \quad (1)$$

Although the values of $t_{0.5}^{-1}$ for releases closely approximate the predicted values, there is a consistent tendency for phase

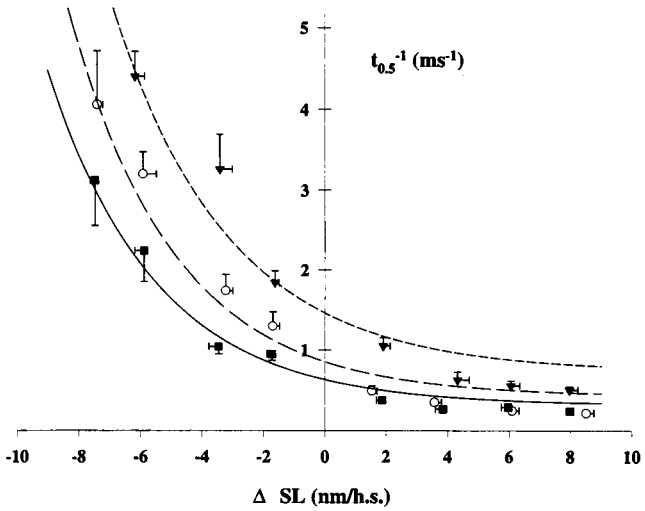


FIGURE 5 The dependence of the rate of tension recovery during phase 2 ($t_{0.5}^{-1}$ (ms$^{-1}$); mean ± SE) upon $\Delta L_S$ was determined at pCa 6.6 (▼, - - - - -), 6.4 (○, – – – –), and 4.0 (■, ——) for seven fibers, as illustrated in Figs. 3 and 4 *C*. The lines represent nonlinear least-squares regression of individual data points from all fibers fit to Eq. 1 at each [$Ca^{2+}$].

2 kinetics obtained with stretches to be slower than the predicted rates, similar to observations obtained in intact tetanized frog fibers (Huxley and Simmons, 1971).

Fig. 6 illustrates the $Ca^{2+}$-activation dependence of the regression estimates for the parameters in Eq. 1 ($k_-$ and $\alpha$) for the data shown in Fig. 5, as well as for one fiber at pCa 6.2. Regressions were performed at each pCa on the individual data points combined from all fibers. The exponential term $\alpha$ was unaffected by activation level, whereas $k_-$ was elevated at low activation.

## DISCUSSION

The results of this study indicate that the rate of tension recovery during phase 2 of force transients varies with $Ca^{2+}$-activation level and is fastest at low levels of steady isometric force. A similar monotonic decline with increasing [$Ca^{2+}$] has also been shown for the rapid process associated with phase 2 (process $2\pi c$) using sinusoidal length perturbations of skinned fibers (Kawai et al., 1981). Our observations in steady-state activations of skinned fibers complement similar measurements made during the rise of tetanic tension in intact fibers (Bagni et al., 1988; Ford et al., 1986) and support the hypotheses that the molecular transitions occurring during phase 2 may be sensitive to either the number of attached actomyosin cross-bridges, [$Ca^{2+}$] per se (i.e., $Ca^{2+}$ binding to sites other than TnC), or the level of thin filament activation.

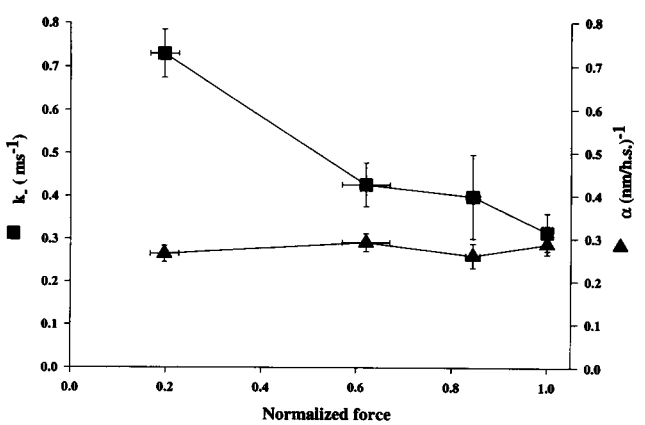


FIGURE 6 $Ca^{2+}$-activation dependence of regression estimates of variable parameters in Eq. 1, $\alpha$ (▲) and $k_-$ (■, obtained from the nonlinear least-squares fits of $t_{0.5}^{-1}$ vs. $\Delta L_S$, as shown in Fig. 5. Data are shown for seven fibers at pCa 6.6, 6.4, and 4.0, and for one fiber at pCa 6.2, in order of increasing normalized force. The error bars indicate SE for the regression parameters and SD for normalized force.

## Characterization of phase 2 kinetics

A model has been proposed that describes the nature of the processes occurring during phase 2, based on the properties of individual cross-bridges, which are assumed to be independent tension generators (Huxley and Simmons, 1971). In this model, during steady-state force production there is an equilibrium distribution between two attached states in which the forward rate constant $k_+$ decreases with increased extension or degree of strain of the attached cross-bridge, whereas the reverse rate constant $k_-$ does not depend on strain. The relation between these rate constants was modeled as $k_+ = k_-(e^{-y \cdot Kh/kT})$ ($y = \Delta L_S$, $K$ is the stiffness of a single cross-bridge, $h$ is the extent of cross-bridge motion associated with the transition, $k$ is the Boltzman constant, and $T$ is absolute temperature), and the rate of transition to a new equilibrium force ($T_2$) was $r = k_+ + k_-$, or equivalently $r = k_- (1 + e^{-y \cdot Kh/kT})$ (Eq. 1).

We have analyzed the activation dependence of $r$ using Eq. 1 (Figs. 5 and 6) and found that $k_-$ depended on the level of activation, whereas $\alpha$ ($=Kh/kT$) did not (Fig. 6). An important feature of the analysis is the case when $\Delta L_S = 0$, $k_+ = k_-$, and the $t_{0.5}^{-1}$ intercept is $2k_-$ (Fig. 5). The $t_{0.5}^{-1}$ intercept is shifted toward higher rates at lower [$Ca^{2+}$], implying that $k_-$ increases at lower activation levels. However, characterization of phase 2 kinetics by a single transition may be an oversimplification because tension recovery during phase 2 appears to be comprised of multiple components (Davis and Harrington, 1993; Ford et al., 1977, 1986; Huxley and Simmons, 1971; Shuman et al., 1991; Zhao and Kawai, 1993). Because of the finite bandwidth of our force transducer, we have not attempted to separate the effects of $Ca^{2+}$ on individual components of phase 2 tension recovery. The apparent slowing of $r$ with increased [$Ca^{2+}$] could arise from a fast phase of recovery that becomes faster as [$Ca^{2+}$] is elevated, to the point of being unresolvable by our apparatus. However, if this were the case, one would expect to observe an increase in $r$ as [$Ca^{2+}$] is increased, followed by a plateau. Instead, there is a monotonic decline of $t_{0.5}^{-1}$, and thus $k_-$, as illustrated in Figs. 5 and 6. Although we cannot absolutely exclude the possibility of a very fast component of tension recovery that has a positive activation dependence, analysis using $t_{0.5}^{-1}$ lumps such processes together and, thus, our data

imply that at least one of these putative components must be faster at low levels of activation.

Interpretation of the results in Figs. 5 and 6 could also be complicated by recent evidence that suggests that up to 20% of the sarcomere compliance at maximal activation could reside in thin filaments (Bagni et al., 1990; Huxley et al., 1994). If this is the case, the change in strain of attached cross-bridges would be overestimated from changes in $L_S$, and the data in Fig. 6 should be shifted toward smaller $\Delta L_S$, with the shift being greater at pCa 4.0. However, the overestimation of the change in cross-bridge strain would be greater for larger $\Delta L_S$ and diminish as $\Delta L_S$ approaches zero, and thus cannot explain the faster rate of phase 2 tension recovery ($t_{0.5}^{-1}$) at submaximal activation (Figs. 5 and 6).

## Interpretation of activation-dependent phase 2 kinetics

The faster kinetics of phase 2 during the rise of tension in a tetanus have been explained by models that involve enhanced flux through early cross-bridge states on the approach to steady-state (Ford et al., 1986). Thus, our steady-state data (Figs. 5 and 6) are not consistent with this explanation. Also, although able to explain the elevated ratio of stiffness to force during the rising phase of a tetanus, this class of model does not predict the increased ratio of stiffness to force during steady-state $Ca^{2+}$-activations (Martyn and Gordon, 1992) unless $Ca^{2+}$-dependent rate constants are specifically incorporated (Ford et al., 1986). As an alternative, the more rapid phase 2 kinetics observed during the rise of tetanic force could result from transitions between weakly and strongly attached cross-bridge states (Brenner, 1990). However, two observations argue against this scheme. First, the population of weakly bound cross-bridges is low in both relaxed and activated fibers at higher ionic strengths (Schoenberg, 1988). Second, stiffness does not change significantly during the phase 2 tension transient (Cecchi et al., 1986; Julian and Morgan, 1981), indicating that the distribution of cross-bridges between weak and strong binding states does not change during phase 2.

The Huxley and Simmons (1971) model has been extended to explain the constant relation between force and stiffness over a wide range of conditions and the faster phase 2 kinetics during the rise of force in a tetanus (Bagni et al., 1988). This expanded model incorporates positive cooperative interactions between cross-bridges, such that an increase in the population of attached cross-bridges causes an increase in the energy barrier for the transition of state 2 to state 1, resulting in a decrease in $k_-$ and thus slowing of phase 2. Conversely, at low activation the transition from state 2 to state 1 is more likely to occur, thus shifting the population of attached cross-bridges toward state 1. Although this model is attractive because it explains results obtained under a wide variety of conditions, it may not accurately predict an elevation of stiffness relative to force at threshold force levels, as observed by Ford et al. (1986). However, our data (Fig. 6) are consistent with the model of Bagni et al. (1988) and extend the range of observations that can be explained in this manner to include the relationship between phase 2 kinetics and force during steady-state contractions. Our previous observation that the ratio of stiffness to force is elevated at submaximal isometric force levels relative to maximal activation (Fig. 4 *B*) (Martyn and Gordon, 1992) is also consistent with this proposition. In the same context, the observation that $\alpha$ is strikingly independent of activation (Fig.6) implies, because the product $Kh$ is constant, either that these properties of individual cross-bridges ($K$ and $h$) are unaffected by activation or that they vary by equal but opposite amounts.

Possible pathways for the interactions between attached cross-bridges implied by this model might include those between cross-bridges and thin filament regulatory units, conformational changes in myosin-binding sites on actin caused by thin filament strain, or direct interactions between adjacent attached myosin heads. These possibilities are supported by observations that imply thin filament elasticity (Bagni et al., 1990), cross-bridge binding to more than one actin subunit (Andreeva et al., 1993; Mornet et al., 1981; Rayment et al., 1993a; Rayment et al., 1993b), and possible direct interaction sites between myosin and tropomyosin or between adjacent myosins (Rayment et al., 1993a; Schröder et al., 1993).

Our results do not allow us to determine whether $Ca^{2+}$-binding or thin filament activation directly affects the kinetics of individual cross-bridges during phase 2 tension recovery, or whether cooperative cross-bridge interactions are the primary modulatory mechanism. However, they do suggest that kinetics of the elementary force-generating transition vary inversely with the level of contractile activation, which can be modeled by a slower reverse transition rate as activation increases, thus effectively stabilizing cross-bridges in states that produce higher force.

The authors would like to thank Dr. T. W. Beck, Robin Coby, Martha Mathiason, and Donald Anderson for technical assistance and Drs. A. M. Gordon, M. J. Kushmerick, and M. Schoenberg for helpful comments.
This work was supported by National Institutes of Health grants HL-31962 and NS-08384.

## REFERENCES

Andreeva, A. L., O. A. Andreev, and J. Borejdo. 1993. Structure of the 265-kilodalton complex formed upon EDC cross-linking of subfragment 1 to F-actin. *Biochemistry.* 32:13956–13960.

Bagni, M. A., G. Cecchi, F. Colomo, and C. Poggesi. 1990. Tension and stiffness of frog muscle fibres at full filament overlap. *J. Muscle Res. Cell Motil.* 11:371–377.

Bagni, M. A., G. Cecchi, and M. Schoenberg. 1988. A model of force production that explains the lag between crossbridge attachment and force after electrical stimulation of striated muscle fibers. *Biophys. J.* 54:1105–1114.

Brenner, B. 1983. Technique for stabilizing the striation pattern in maximally calcium-activated skinned rabbit psoas fibers. *Biophys. J.* 41: 99–102.

Brenner, B. 1990. Muscle mechanics and biochemical kinetics. *In* Molecular Mechanisms in Muscular Contraction. J. M. Squire, editors. CRC Press, Boca Raton, FL. 77–149.

Brenner, B., and L. C. Yu. 1985. Equatorial x-ray diffraction from single skinned rabbit psoas fibers at various degrees of activation. *Biophys. J.* 48:829–834.

Cecchi, G., P. J. Griffiths, and S. Taylor. 1986. Stiffness and force in activated frog skeletal muscle fibers. *Biophys. J.* 49:437–451.

Chase, P. B., T. W. Beck, J. Bursell, and M. J. Kushmerick. 1991. Molecular charge dominates the inhibition of actomyosin in skinned muscle fibers by $SH_1$ peptides. *Biophys. J.* 60:352–359.

Chase, P. B., and M. J. Kushmerick. 1988. Effects of pH on contraction of rabbit fast and slow skeletal muscle fibers. *Biophys. J.* 53:935–946.

Chase, P. B., D. A. Martyn, M. J. Kushmerick, and A. M. Gordon. 1993. Effects of inorganic phosphate analogues on stiffness and unloaded shortening of skinned muscle fibres from rabbit. *J. Physiol. (Lond.).* 460: 231–246.

Davis, J. S., and W. F. Harrington. 1993. A single order-disorder transition generates tension during the Huxley-Simmons phase 2 in muscle. *Biophys. J.* 65:1886–1898.

Ford, L. E., A. F. Huxley, and R. M. Simmons. 1977. Tension responses to sudden length change in stimulated frog muscle fibres near slack length. *J. Physiol. (Lond.).* 269:441–515.

Ford, L. E., A. F. Huxley, and R. M. Simmons. 1986. Tension transients during the rise of tetanic tension in frog muscle fibres. *J. Physiol. (Lond.).* 372:595–609.

Goldman, Y. E. 1987. Measurement of sarcomere shortening in skinned fibers from frog muscle by white light diffraction. *Biophys. J.* 52:57–68.

Goldman, Y. E., and R. M. Simmons. 1984. Control of sarcomere length in skinned muscle fibres of *Rana temporaria* during mechanical transients. *J. Physiol. (Lond.).* 350:497–518.

Goldman, Y. E., and R. M. Simmons. 1986. The stiffness of frog skinned muscle fibres at altered lateral filament spacing. *J. Physiol. (Lond.).* 378: 175–194.

Huxley, A. F., and R. M. Simmons. 1971. Proposed mechanism of force generation in striated muscle. *Nature.* 233:533–538.

Huxley, H., A. Stewart, H. Sosa, and T. Irving. 1994. X -ray diffraction measurements of the extensibility of the actin and myosin filaments in muscle. *Biophys. J.* 66:191*a*. (Abstr.)

Irving, M. 1993. Birefringence changes associated with isometric contraction and rapid shortening steps in frog skeletal muscle fibres. *J. Physiol. (Lond.).* 472:127–156.

Irving, M., V. Lombardi, G. Piazzesi, and M. A. Ferenczi. 1992. Myosin head movements are synchronous with the elementary force-generating process in muscle. *Nature.* 357:156–158.

Julian, F. J., and D. L. Morgan. 1981. Variation of muscle stiffness with tension during tension transients and constant velocity shortening in the frog. *J. Physiol. (Lond.).* 319:193–203.

Kawai, M., P. W. Brandt, and M. Orentlicher. 1977. Dependence of energy transduction in intact skeletal muscles on the time in tension. *Biophys. J.* 18:161–172.

Kawai, M., R. N. Cox, and P. W. Brandt. 1981. Effect of Ca ion concentration on cross-bridge kinetics in rabbit psoas fibers. Evidence for the presence of two Ca-activated states of thin filament. *Biophys. J.* 35: 375–384.

Kawai, M., J. S. Wray, and Y. Zhao. 1993. The effect of lattice spacing change on cross-bridge kinetics in chemically skinned rabbit psoas muscle fibers. I. Proportionality between the lattice spacing and the fiber width. *Biophys. J.* 64:187–196.

Lombardi, V., G. Piazzesi, and M. Linari. 1992. Rapid regeneration of the actin-myosin power stroke in contracting muscle. *Nature.* 355:638–641.

Martyn, D. A., P. B. Chase, T. W. Beck, M. J. Kushmerick, and A. M. Gordon. 1994. Force dependence of phase 2 tension recovery with altered calcium or phosphate analog inhibitors of skinned skeletal muscle. *Biophys. J.* 66:302*a*. (Abstr.)

Martyn, D. A., and A. M. Gordon. 1988. Length and myofilament spacing-dependent changes in calcium sensitivity of skeletal fibres: effects of pH and ionic strength. *J. Muscle Res. Cell Motil.* 9:428–445.

Martyn, D. A., and A. M. Gordon. 1992. Force and stiffness in glycerinated rabbit psoas fibers. Effects of calcium and elevated phosphate. *J. Gen. Physiol.* 99:795–816.

Matsubara, I., Y. Umazume, and N. Yagi. 1985. Lateral filamentary spacing in chemically skinned murine muscles during contraction. *J. Physiol. (Lond.).* 360:135–148.

Mornet, D., R. Bertrand, P. Pantel, E. Audemard, and R. Kassab. 1981. Structure of the actin-myosin interface. *Nature.* 292:301–306.

Rayment, I., H. M. Holden, M. Whittaker, C. B. Yohn, M. Lorenz, K. C. Holmes, and R. A. Milligan. 1993a. Structure of the actin-myosin complex and its implications for muscle contraction. *Science.* 261:58–65.

Rayment, I., W. R. Rypniewski, K. Schmidt-Bäse, R. Smith, D. R. Tomchick, M. M. Benning, D. A. Winkelmann, G. Wesenberg, and H. M. Holden. 1993b. Three-dimensional structure of myosin subfragment-1: a molecular motor. *Science.* 261:50–58.

Schoenberg, M. 1988. Characterization of the myosin adenosine triphosphate (M·ATP) crossbridge in rabbit and frog skeletal muscle fibers. *Biophys. J.* 54:135–148.

Schröder, R. R., D. J. Manstein, W. Jahn, H. Holden, I. Rayment, K. C. Holmes, and J. A. Spudich. 1993. Three-dimensional atomic model of F-actin decorated with *Dictyostelium* myosin S1. *Nature.* 364:171–174.

Seow, C. Y., and L. E. Ford. 1993. High ionic strength and low pH detain activated skinned rabbit skeletal muscle crossbridges in a low force state. *J. Gen. Physiol.* 101:487–511.

Shuman, H., J. A. Dantzig, and Y. E. Goldman. 1991. Computer simulations of mechanical transients in skeletal muscle fibers. *The Physiologist.* 34: 116*a*. (Abstr.)

Sweeney, H. L., S. A. Corteselli, and M. J. Kushmerick. 1987. Measurements on permeabilized skeletal muscle fibers during continuous activation. *Am. J. Physiol.* 252:C575–C580.

Zhao, Y., and M. Kawai. 1993. The effect of lattice spacing change on cross-bridge kinetics in chemically skinned rabbit psoas muscle fibers. I. Elementary steps affected by the spacing change. *Biophys. J.* 64:197–210.

Zite-Ferenczy, F., K.-D. Haberle, R. Rudel, and W. Wilke. 1986. Correlation between the light diffraction pattern and the structure of a muscle fibre realized with Ewald's construction. *J. Muscle Res. Cell Motil.* 7:197–214.